Journal of Geological Socicty of Sri Lanka Vol. 12 (2007), 27-35

REACTIVE FLUID TRANSPORT MODELING OF REMOVAL OF EXCESS NITRATE FROM GROUNDWATER BY PYRITE OXIDATION

NISHANTHA ATTANAYAKE[1,2] AND LUKAS BAUMGARTNER[3]

[1] Institute of Geosciences, Johannes Gutenberg University of Mainz, D-55099 Mainz, Germany

Present Address: [2] Geological Survey and Mines Bureau, 4, Galle Road, Dehiwala, Sri Lanka: Email: attanayake@gsmb.gov.lk

[3] Institute of Mineralogy and Geochemistry, BFSH2, University of Lausanne, CH-1015 Lausanne, Switzerland

ABSTRACT

The use of permeable reactive barriers has proven to be an efficient method in removing certain groundwater contaminants. For such installations to be cost effective, it is important to predict their performance prior to implementation. Reactive fluid transport models can provide valuable information in this regard. A case of nitrate removal from groundwater was modeled by reducing it to nitrogen through oxidation by an iron-bearing mineral, pyrite. A one-dimensional reactive fluid transport code, 1DREACT was used to simulate the pyrite oxidation reaction taking place in a hypothetical denitrification wall. Simulations show that nitrate concentration in groundwater can be lowered by a factor of 3 within a week. Although sulphate concentration increases due to dissolution of pyrite, it can be maintained at values below the recommended level for drinking water. Fluid flow rate and pyrite reactive surface area are the major factors that control the efficiency of nitrate removal.

INTRODUCTION

Numerous studies have demonstrated the potential of reactive fluid transport models to assess the physical, geochemical and biological processes involved in contaminated groundwater transport and treatment (Baveye and Valocchi, 1989; Hunter et al., 1998; Rosqvist and Destouni, 2000; MacQuarrie and Sudicky, 2001; Liedl and Ptak, 2003). They couple the hydrological properties of the subsurface with geochemical reactions occurring between the fluid and the minerals of the aquifers. Hence proposed scenarios of groundwater remediation can be cost efficiently modeled, in order to design optimized rectifying measures for contaminated aquifers. The necessity for such exercises is becoming significant with the ever increasing threats for groundwater quality. Industries, agriculture and waste disposal are the main contributors for groundwater contamination. The types of pollutants are wide and varied, and so is their behaviour in aquifers.

Among many groundwater contaminants, nitrate (NO_3^-) is a common solute that propagates into aquifers from agricultural lands as it is a major component in fertilizers and manure. Also domestic and urban sewage are responsible for extensive release of nitrate into groundwater systems. Although nitrate is found naturally at moderate concentrations in most of the aquatic systems, its enrichment in subsurface water bodies poses a threat to drinking water supplies due to its carcinogenic nature. The maximum admissible NO_3^- concentration in drinking water is 50 mg/l while the recommended level is 25 mg/l according to World Health Organization (WHO) standards (Appelo and Postma, 1999). In aquatic systems nitrate does not form any mineral that can be precipitated. Nor is it adsorbed onto any aquifer material as far as it is known today. Therefore the only means for its removal from groundwater is by reduction. Several methods are being employed in nitrate removal from groundwater. Organic matter has the potential for reducing NO_3^- to N_2 in a bacterially catalyzed reaction. This denitrification process is commonly used in field scale implementations (eg. Schipper and others, 2004). Jørgensen and others (2004) give a detailed account on the natural denitrification by bacteria mediated reactions in saturated aquifers consisting of organic-rich clays. Another process of NO_3^- reduction in aquifers is by ferrous to ferric oxidation of iron. A typical source of Fe^{2+} in an aquifer can be Fe (II)-bearing minerals (Appelo and Postma, 1999). A well known process of NO_3^- removal is by pyrite oxidation (Postma and others, 1991) and will be the subject of the following discussion. This involves oxidation of both Fe(II) and sulfur and can be described by the following reaction (Appelo and Postma, 1999).

$$5\ FeS_2\ (pyrite) + 14\ NO_3^- + 4\ H^+ = 7\ N_2(g) + 10\ SO_4^{2-} + 5\ Fe^{2+} + 2\ H_2O \quad (1)$$

It is apparent that introducing pyrite into the flow path might help lower the NO_3^- concentration by reducing it to nitrogen. Postma et al. (1991) have illustrated the expected increase in SO_4^{2-} and Fe^{2+} with field examples. However if SO_4^{2-} and Fe^{2+} concentrations in the solution can still be maintained below the maximum admissible levels for drinking water, this process may successfully be employed for NO_3^- removal by installing a pyrite-bearing zone across the flow path in the form of a denitrification wall. Permeable reactive barriers have been in use and reported to be efficiently removing NO_3^- from groundwater, in some cases in excess of 90% (Robertson and Cherry, 1995; Robertson and others, 2000; Schipper and Vojvodic-Vokovic, 2000). This paper discusses the simulation of the above geochemical reaction using the reactive fluid transport code 1DREACT (Steefel, 1993) in order to design an optimum condition under which the NO_3^- concentration could be minimized. The reaction in Equation 1 is best known to take place under anoxic conditions and particularly mediated by microbial activity. However the simulations will be carried out considering only the geochemical aspects as provisions to accommodate microbial reactions are not available in the present code.

Reactive fluid transport modeling

The coupled reaction and transport equation for the conservation of mass of a solute species can be expressed as (Steefel, 1993),

$$\frac{\partial(\varphi C_i)}{\partial t} + \nabla.(uC_i - D\nabla C_i) = R_j \quad (j = 1, \ldots N_c) \qquad (2)$$

where φ is the porosity, C_j is the total concentration of the j^{th} species, u is the Darcian fluid flux, D is the combined dispersion/diffusion coefficient and R_j is the total rate of the heterogeneous mineral-fluid reactions affecting the concentration of j^{th} species in solution. N_c is the total number of components. The total concentration is the sum of concentrations of species in the fluid phase for each component j. Equation 2, when implemented with a suitable numerical algorithm, provides a tool to describe many of the processes that involve chemical reactions and fluid transport in geologic media.

Fluid-rock interaction simulations are carried out using the one dimensional multicomponent reactive fluid transport code, 1DREACT (Steefel, 1993; Steefel and Lasaga, 1994) which is based on an integrated finite difference formulation of Eqn. 2 that solves for aqueous species concentrations, calculates mineral precipitation/dissolution rates, saturation states, and mineral volumes for systems with diffusion and infiltration. It requires a thermodynamic database, initial fluid composition, mineral abundances and the physical transport parameters of the flow system.

Model parameters

A 2 m long one-dimensional section of a hypothetical aquifer which consists of sandy-clayey material was taken as the model domain. Mineral volume percentages were assigned (25% kaolinite, 40% quartz) such that a high porosity (35%) is allowed. A permeable reactive barrier zone consisting of pyrite (15%) together with other aquifer material (10% kaolinite, 40% quartz) was introduced into the flow path (Fig. 1). The grid was discretized into 1 cm segments for transport calculations. The initial composition of the water entering the model domain was taken to be in the range of solute concentrations of the influent solution used by Jørgensen and others (2004) in their experiments on nitrate removal by organic matter (Table 1). Additionally an artificial concentration of NO_3^- (70 mg/l) was introduced. Initial chemical speciation of the water flowing into the pyrite barrier zone and that of the water leaving it after reacting with pyrite were calculated using the geochemical model PHREEQC (Parkhurst and Appelo, 1999). These compositions were used to initialize the model grid as shown in Table 2 for the transport calculations with 1DREACT.

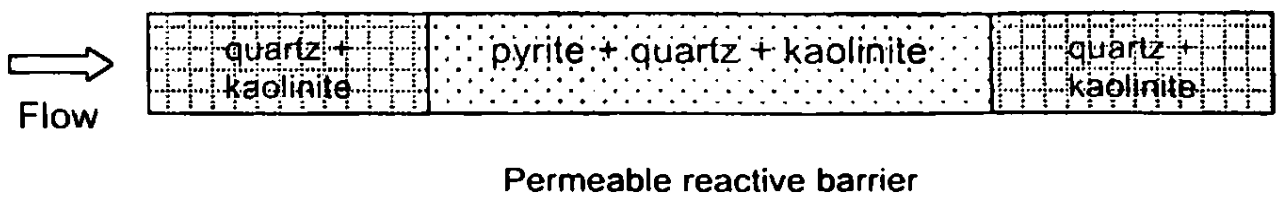

Fig: 1. One-dimensional model grid. Pyrite-bearing zone acts as a permeable reactive barrier.

Table 1. *Chemical composition of the groundwater used in simulations.*

Component	Concentration (ppm)
Na	60
K	5
Ca	95
Mg	23
NO_3^-	70*
SO_4^{-2}	20
HCO_3^-	380
pH	7.8

* introduced concentration

Dispersivity of the medium was taken as 0.03 m while a value of 1 x 10^{-9} m^2s^{-1} was assigned for the diffusion coefficient for all solute species. Dissolution/precipitation rates of minerals and the activation energies used in the simulations are given in Table 3. For those minerals where experimental data are not available the reaction rates were assumed to be 1 x 10^{-9} moles $m^{-2}s^{-1}$ at 25 °C. The thermodynamic database used by 1DREACT for mineral-fluid reaction calculations contains log*K*'s of hydrolysis reactions of minerals and aqueous complexes. Log*K* of the reaction in Equation 1 as written for one mole of reacting pyrite at 25 °C was calculated (211.027) using SUPCRT92 (Johnson et al., 1992) and included in the thermodynamic database. Simulations were carried out for different mineral surface areas, lengths of the reactive barrier zone and flow rates.

Table 2. *Initial fluid compositions distributed along the model grid, and the constraints used to buffer the aqueous species concentrations.*

Component	Concentration (mol/kg w)		
	Fluid inlet	Fluid outlet	Constraint
H^+	1.747×10^{-08}	8.445×10^{-09}	Charge balance
$Al(OH)_4^-$	1.000×10^{-12}	1.900×10^{-07}	Total Al concentration
Ca^{+2}	2.167×10^{-03}	2.035×10^{-03}	Total Ca concentration
Fe^{+2}	1.000×10^{-12}	1.874×10^{-04}	Total Fe concentration
HCO_3^-	7.238×10^{-03}	7.095×10^{-03}	Total C concentration
K^+	1.279×10^{-04}	1.275×10^{-04}	Total K concentration
Mg^{+2}	8.734×10^{-04}	8.192×10^{-04}	Total Mg concentration
Na^+	2.601×10^{-03}	2.595×10^{-03}	Total Na concentration
NO_3^-	1.130×10^{-03}	1.000×10^{-10}	Total N(V) concentration
SO_4^{-2}	1.633×10^{-04}	8.011×10^{-04}	Total S(VI) concentration
$SiO_2(aq)$	1.000×10^{-05}	1.000×10^{-05}	Total SiO_2 concentration
$N_2(g)$	1.000×10^{-15}	1.000×10^{-10}	Total N(III) concentration

Table 3. *Reaction rates and activation energies of minerals used in simulations.*

Mineral	Reaction rate at 25°C (mol/m^2/s)	Activation energy (kcal/mol)	Comments
Calcite	1.0000×10^{-09}	15.0	Assumed value
Gibbsite	3.5481×10^{-12}	15.0	Data from Lasaga (1998)
Gypsum	1.0000×10^{-09}	15.0	Assumed value
Kaolinite	5.2480×10^{-14}	16.0	Data from Lasaga (1998)
Pyrite	1.0000×10^{-09}	15.0	Assumed value
Quartz	4.0738×10^{-14}	17.0	Data from Lasaga (1998)

Results and discussion

Since the reaction in Equation 1 is known to take place under anoxic conditions, reactive fluid flow modeling was carried out in the saturated zone of the aquifer. Figure 2 shows the change in NO_3^- concentration along the model grid after one week. When an average groundwater flow rate of 150 m yr^{-1} and a 2.0 m long pyrite zone with silt-sized particles were used, the system approached the steady state in one week. NO_3^- concentration was lowered to about 20 ppm in the effluent solution, which is a significant decrease from the initial ~70 ppm (70 mg/l). With higher flow rates the system approaches steady state in one week, but the decrease in NO_3^- concentration is small (Fig. 3).

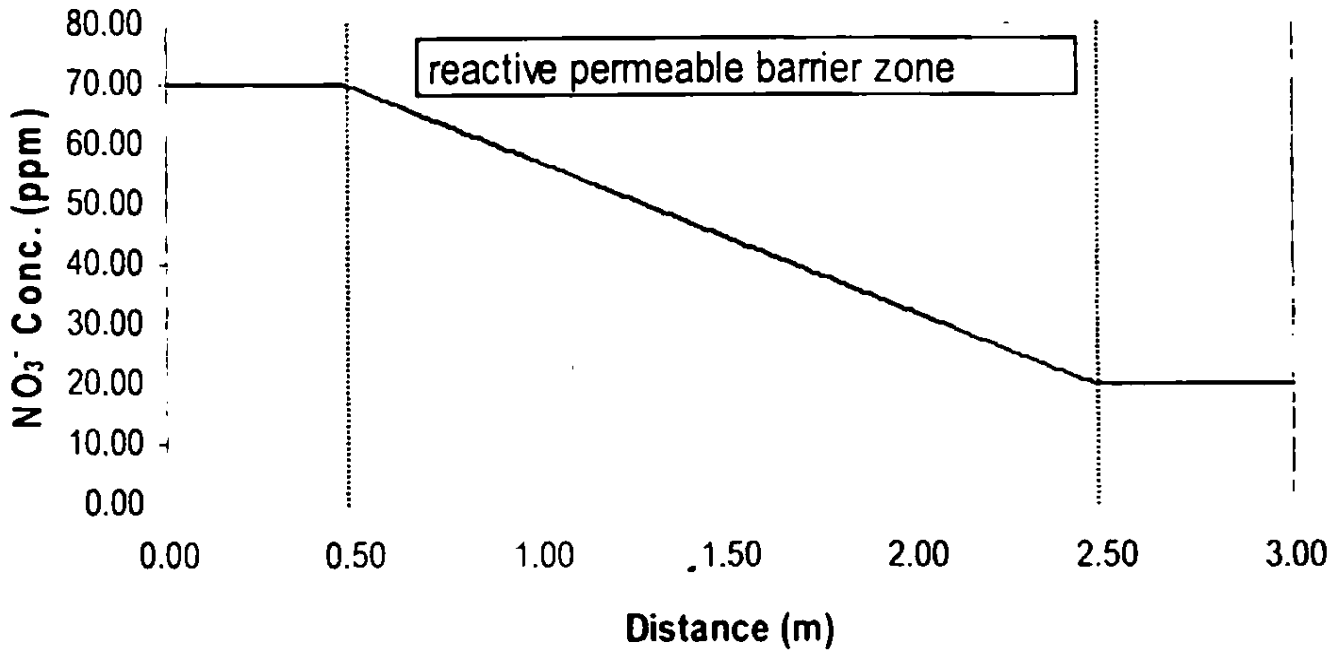

***Fig:** 2. Change of NO_3^- concentration along the model grid when a flow rate of 150 m yr^{-1} is used.*

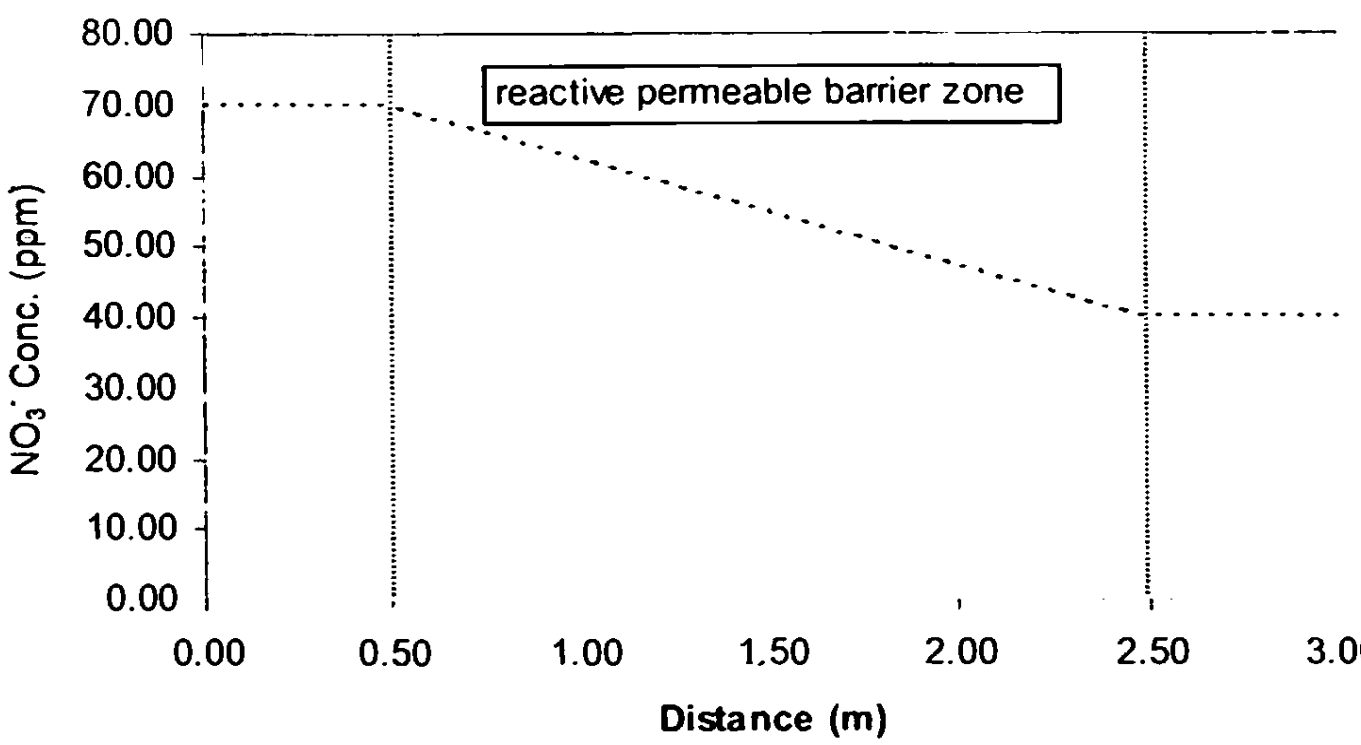

***Fig:** 3. Change of NO_3^- concentration along the model grid when a flow rate of 250 m yr^{-1} is used.*

Change of SO_4^{-2} concentration along the grid is shown in Figure 4. It can be observed that SO_4^{-2} concentration in the effluent has almost the inverse relation to NO_3^- concentration as 2.8 moles of NO_3^- are consumed to produce 2 moles of SO_4^{-2}. Since Ca^{+2} in the water is continuously being removed by precipitation of minor amount of calcite (Fig. 5), SO_4^{-2} remains in the aqueous phase due to unavailability of cations to form a precipitate. However, the steady state concentration of SO_4^{-2}, as

shown in Figure 4, is 63 ppm which is reasonable and well below the maximum permissible level for drinking water (250 mg/l according to WHO standards). Major concentration changes in aqueous species after passing the denitrification wall can be observed in NO_3^-, SO_4^{-2}, Ca^{+2}, HCO_3^- and Fe^{+2} (Fig. 6). Slight decrease in pH (Fig. 7) can be attributed to the addition of H^+ by the reaction between Ca^{+2} and HCO_3^- to form calcite.

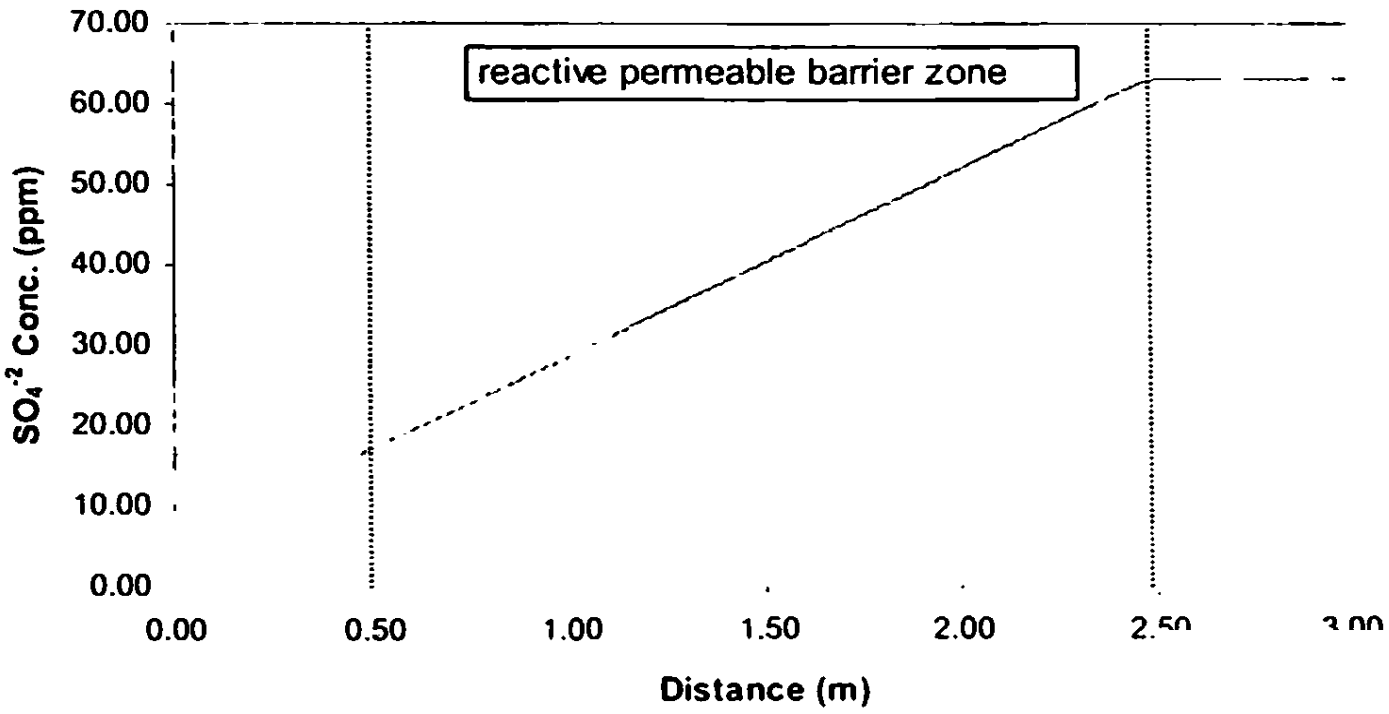

Fig: 4. Change of SO_4^{-2} concentration along the model grid.

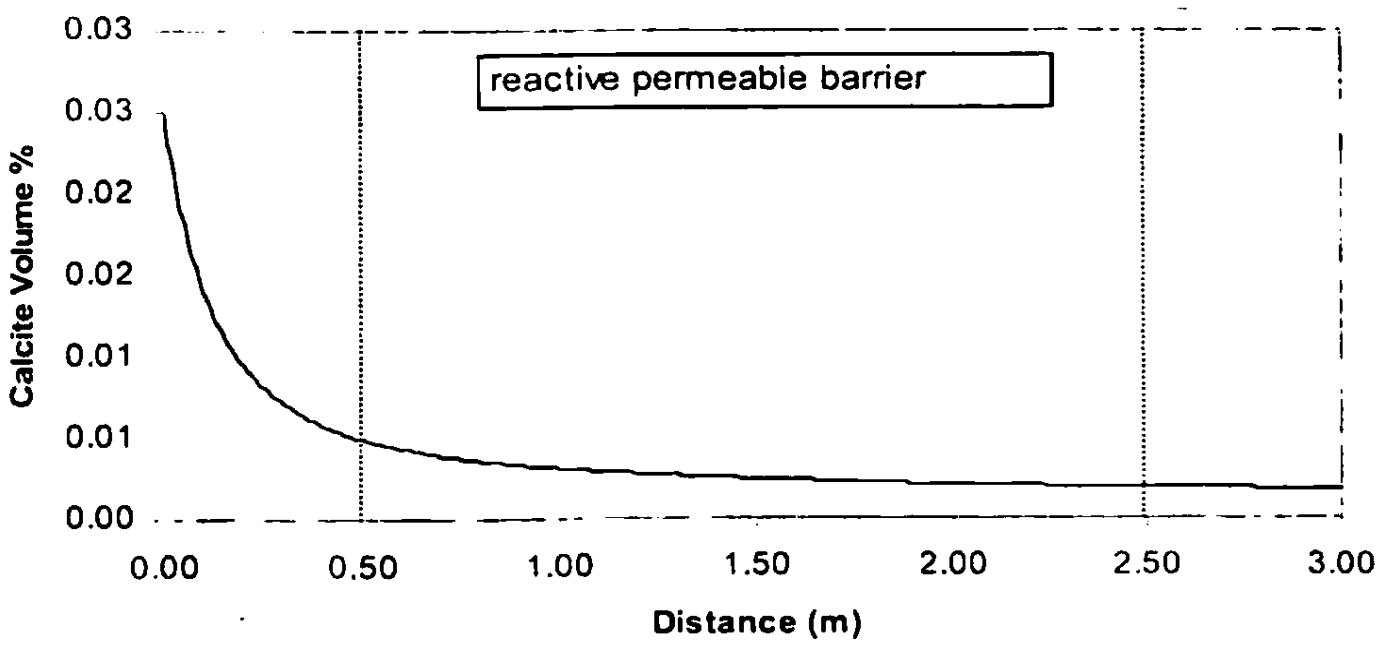

Fig: 5. Calcite precipitation due to fluid-rock interaction.

Reactive surface areas of minerals control the kinetics of mineral-fluid interactions. Therefore tests were carried out changing the pyrite reactive surface areas in order to determine their influence on NO_3^- removal. However, mineral reactive surface areas are not well known (Steefel and Van Cappellen, 1990). Effective reactive surface area can be much less than that of experimentally estimated values as constrained by the connectivity of pore spaces. Assuming fine sand to silt sized spherical grains, surface areas of pyrite were approximated to be in the range of 300 - 700 m^2 per 1 m^3 of the medium. Figure 8 shows the effect of pyrite reactive surface area on the efficiency of NO_3^- removal. As expected, larger reactive surface areas, hence finer particles lowered the NO_3^- concentration significantly. Similar effect can be observed if the length of the pyrite zone is increased for a fixed mineral surface area.

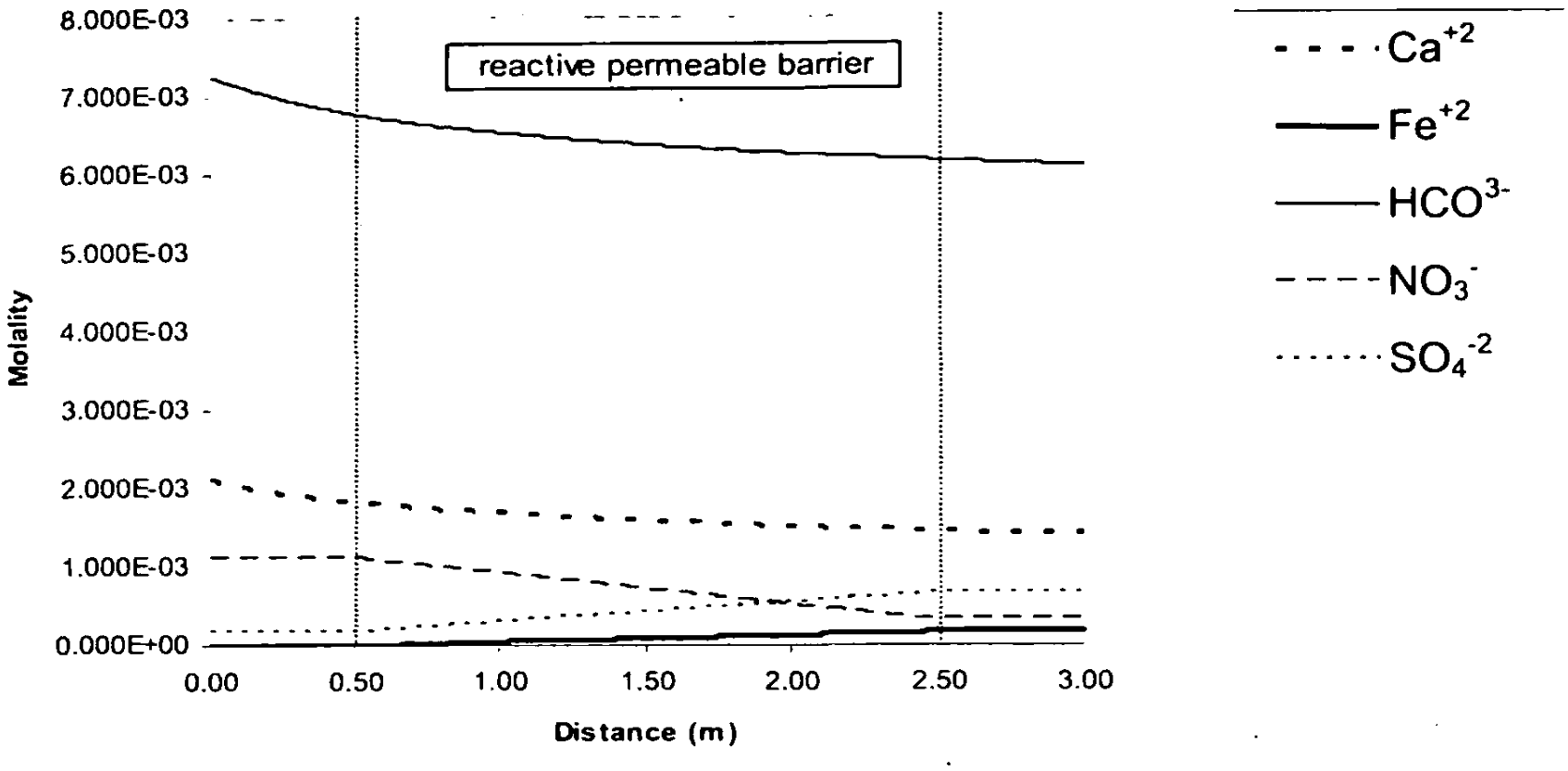

Fig: *6. Aqueous species concentrations along the model grid.*

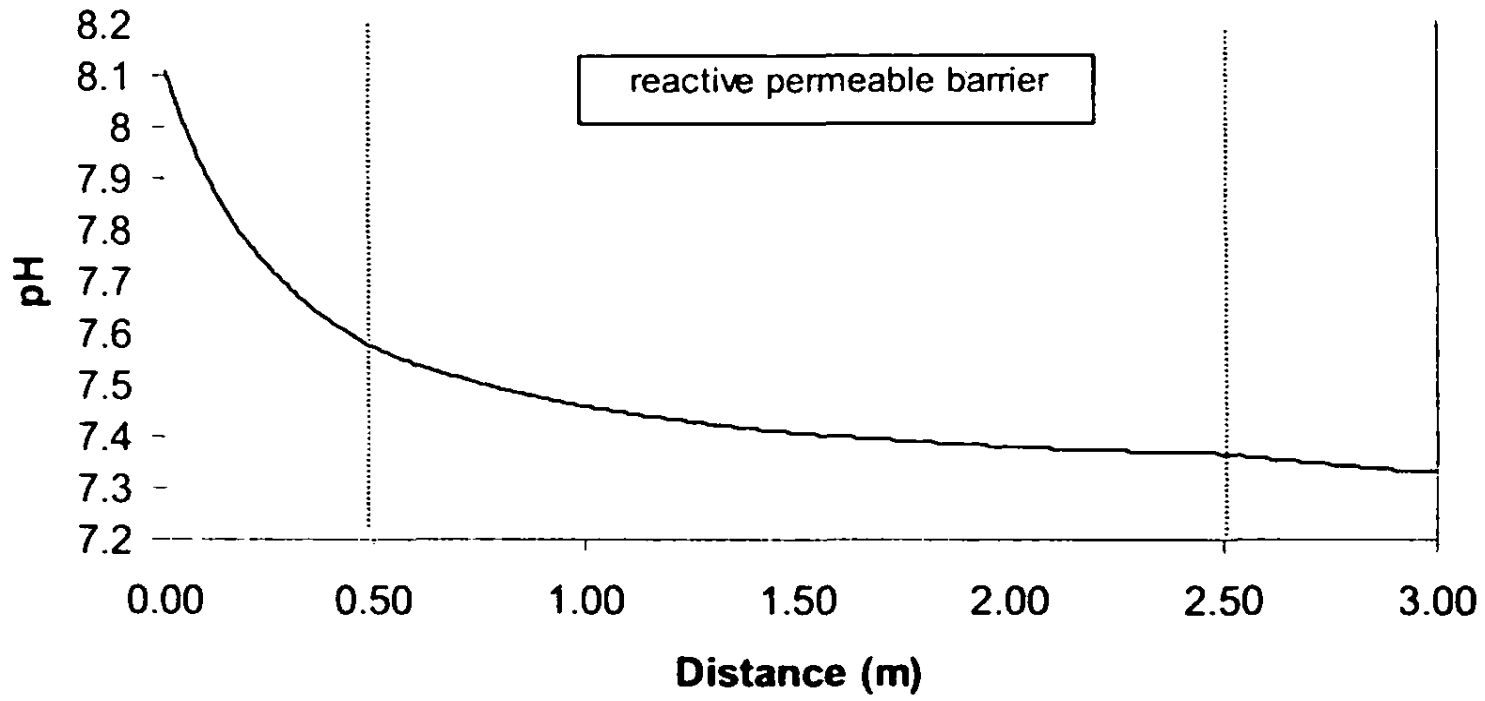

Fig: *7. Change of pH along the model grid.*

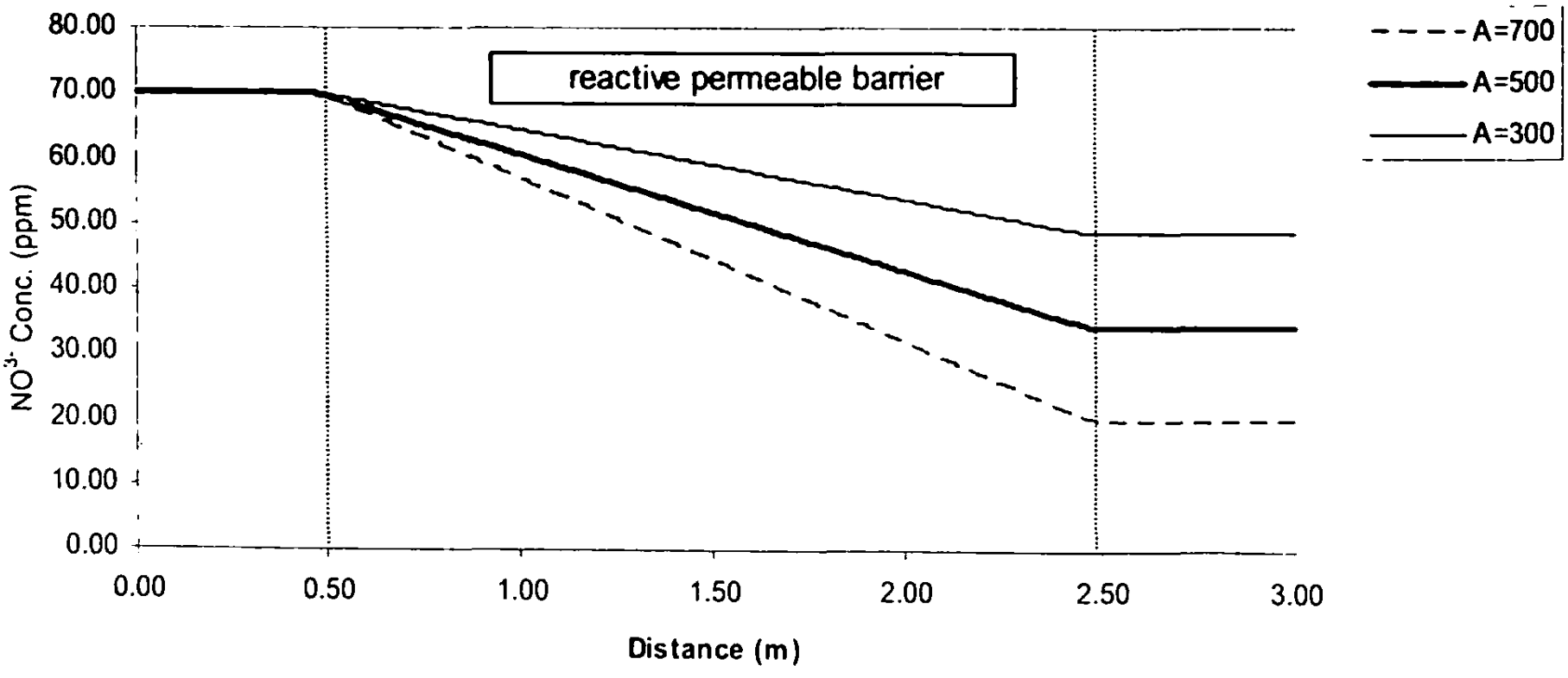

Fig: *8. Effect of pyrite reactive surface area on NO_3^- removal.*

CONCLUSION

Reactive fluid transport calculations have simulated the reduction of NO_3^- to $N_2(g)$ by pyrite oxidation. Since this process takes place under anaerobic conditions, modeling was carried out in a subsurface environment using a permeable reactive barrier consisting of pyrite and sand. It is predicted that this setup is viable. Tests with different reactive surface areas and flow rates show the kinetic control on NO_3^- removal capacity. Flow rate was taken as a variable in simulations to show its effect on NO_3^- removal. However in groundwater environments it is dependent on the natural conditions, and can be considered as constant over short distances and short time periods. Therefore when pyrite-bearing permeable reactive barriers are installed in the groundwater flow paths in aquifers, efficiency of denitrification is controlled by the reactive surface area of pyrite and the length of the reacting zone. Increase in SO_4^{-2} concentration due to dissolution of pyrite can be maintained below the permissible levels for drinking water.

ACKNOWLEDGMENT

Financial assistance to the first author from the Deutsche Forschungsgemeinschaft (DFG) through a Graduate College Fellowship at the University of Mainz, Germany where this research was carried out is thankfully acknowledged.

REFERENCES

Appelo, C.A.J. and Postma, D. (1999) Geochemistry, Groundwater and Pollution. A.A. Balkema, Rotterdam, 536pp.

Bayeve, P. and Valocchi, A. (1989) An evaluation of mathematical models of the transport of biologically reacting solutes in saturated soils and aquifers. Water Resour. Res., vol. 25(6), 1413–1421.

Hunter, K.S., Wang, Y., Van Cappellen, P., (1998) Kinetic modeling of microbially driven redox chemistry of subsurface environments: coupling transport, microbial metabolism and geochemistry. J. Hydrol. vol. 209, 53–80.

Johnson, J.W., Oelkers, E.H. and Helgeson, H.C. (1992) SUPCRT92: A software package for calculating the standard molal thermodynamic properties of minerals, gases, aqueous species, and reactions from 1 to 5000 bars and 0 to 1000 degrees C. Computers & Geosciences, vol. 18(7), 899-947.

Jørgensen, P.R., Urup, J., Helstrup, T., Jensen, M.B., Eiland, F. and Vinther, F.P., (2004) Transport and reduction of nitrate in clayey till underneath forest and arable land. J. Contam. Hydrol. vol. 73, 207– 226.

Lasaga, A.C., 1998. Kinetic theory in the earth sciences. Princeton University Press. 728pp.

Liedl, R. and Ptak, T. (2003) Modelling of diffusion-limited retardation of contaminants in hydraulically and lithologically nonuniform media. J. Contam. Hydrol. vol. 66, 239– 259.

MacQuarrie, K.T.B. and Sudicky, E.A. (2001) Multicomponent simulation of wastewater-derived nitrogen and carbon in shallow unconfined aquifers I. Model formulation and performance. J. Contam. Hydrol. vol. 47, 53–84.

Parkhurst, D.L. and Appelo, C.A.J. (1999) User's guide to PHREEQC (Version 2) - A computer program for speciation, batch-reaction, one-dimensional transport, and inverse geochemical calculations. USGS Water-Resources Investigations Report 99-4259, 312pp.

Postma, D., Boesen, C., Kristiansen, H. and Larsen, F. (1991) Nitrate reduction in an unconfined sandy aquifer: Water chemistry, reduction processes, and geochemical modeling. Water Resour. Res. vol. 27, 2027-2045.

Robertson, W.D. and Cherry, J.A. (1995) In situ denitrification of septic-system nitrate using reactive porous media barriers: field trials. Ground Water vol. 33, 99– 111.

Robertson, W.D., Blowes, D.W., Ptacek, C.J. and Cherry, J.A. (2000) Long-term of in situ reactive barriers for nitrate remediation. Ground Water vol. 38, 689– 695.

Rosqvist, H. and Destouni G. (2000). Solute transport through preferential pathways in municipal solid waste. J. Contam. Hydrol. vol. 46, 39–60.

Schipper, L.A., and Vojvodic-Vukovic, M., (2000) Rates of nitrate removal from groundwater and denitrification in a constructed denitrification wall. Ecol. Eng. vol. 14, 269– 278.

Schipper, L.A., Barkle, G.F., Hadfield, J.C., Vojvodic-Vukovic, M. and Burgess, C.P. (2004) Hydraulic constraints on the performance of a groundwater denitrification wall for nitrate removal from shallow groundwater. J. Contam. Hydrol. vol. 69, 263– 279.

Steefel, C.I. (1993) 1DREACT User Manual.

Steefel, C.I., Van Cappellen, P. (1990) A new kinetic approach to modeling water-rock interaction: the role of nucleation, precursors, and Ostwald ripening. Geochim. Cosmochim. Acta, vol. 54, 2657-2677.